Phase transitions and Bose-Einstein condensation in α-nucleon matter

L. M. Satarov,[1,2] I. N. Mishustin,[1,2] A. Motornenko,[1,3] V. Vovchenko,[1,3] M. I. Gorenstein,[1,4] and H. Stoecker[1,3,5]

[1]*Frankfurt Institute for Advanced Studies, D-60438 Frankfurt am Main, Germany*

[2]*National Research Center "Kurchatov Institute" 123182 Moscow, Russia*

[3]*Institut für Theoretische Physik, Goethe Universität Frankfurt, D-60438 Frankfurt am Main, Germany*

[4]*Bogolyubov Institute for Theoretical Physics, 03680 Kiev, Ukraine*

[5]*GSI Helmholtzzentrum für Schwerionenforschung GmbH, D-64291 Darmstadt, Germany*

(Received 9 November 2018; published 19 February 2019)

The equation of state and phase diagram of isospin-symmetric chemically equilibrated mixture of α particles and nucleons N are studied in the mean-field approximation. The model takes into account the effects of Fermi and Bose statistics for N and α, respectively. We use Skyrme-like parametrization of the mean-field potentials as functions of partial densities n_α and n_N, which contain both attractive and repulsive terms. Parameters of these potentials are chosen by fitting known properties of pure N and pure α matter at zero temperature. The sensitivity of results to the choice of the αN attraction strength is investigated. The phase diagram of the $\alpha - N$ mixture is studied with special attention paid to the liquid-gas phase transitions and the Bose-Einstein condensation of α particles. We have found two first-order phase transitions, stable and metastable, which differ significantly by the fractions of α particles. It is shown that states with α condensate are metastable.

DOI: 10.1103/PhysRevC.99.024909

I. INTRODUCTION

At subsaturation densities and low temperatures, nuclear matter has a tendency for clusterization when small and big nucleon clusters are formed under conditions of thermal and chemical equilibria. This state of excited nuclear matter is realized in nuclear reactions at intermediate energies known as multifragmentation of nuclei [1]. It is believed that clusterized nuclear matter is also formed in outer regions of neutron stars and in supernova explosions [2]. It may play an important role by providing "seed" nuclei for later nucleosynthesis.

Different models have been used to describe the clusterized nuclear matter. In particular, the statistical approach turned out to be very successful to explain the mass and energy distributions of fragments and hadrons produced in heavy-ion collisions, see, e.g., Refs. [3,4]. Another powerful method is to perform molecular-dynamical simulations in a box taking into account effective interactions between nucleons as was done, e.g., in Ref. [5].

To better understand properties of clusterized nuclear matter, one should use more realistic interactions between different clusters and take into account phenomenological constraints. In our recent paper [6], we studied the equation of state (EoS) of an idealized system composed entirely of α particles. Their interaction was described by a Skyrme-like mean-field potential. We have found that such a system exhibits two interesting phenomena, namely, the Bose-Einstein condensation (BEC) and the liquid-gas phase transition (LGPT). Earlier, the cold α matter has been considered microscopically by using phenomenological $\alpha\alpha$ potentials in Refs. [7–9], the lattice calculations were performed in Ref. [10], and the relativistic mean-field (RMF) approach was applied in Ref. [11]. Properties of cold α chains have been discussed in Refs. [12–14].

However, by introducing such a one-component system, one disregards a possible dissociation of α's into lighter clusters and nucleons. This process should be important at nonzero temperatures and large enough baryon densities. Binary $\alpha - N$ matter in chemical equilibrium with respect to reactions $\alpha \leftrightarrow 4N$ has been considered in Ref. [15] by using the virial approach. One should have in mind that the results of Ref. [15] may be justified only at small baryon densities. The two-component van der Waals model with excluded-volume repulsion has been developed to describe properties of $\alpha - N$ mixture in Ref. [16]. Note that both these approaches disregard possible BEC phenomena.

The EoS of matter composed of nucleons and nuclear clusters have been considered within different approaches including the liquid-drop model [2], several versions of the statistical model [17–19] and the RMF models [20–22]. In particular, in Ref. [21], the RMF calculations have been performed with the medium-dependent binding energy of α's. Comparison of the excluded-volume and virial EoSs has been made in Ref. [23]. However, all these models do not include a possibility of BEC. This phenomenon was considered within the quasiparticle approach of Ref. [24] but only for dilute (nearly ideal-gas) mixtures of nucleons and nuclear clusters.

In the present paper, we consider the isospin-symmetric $\alpha - N$ matter under the conditions of chemical equilibrium. The EoS of such matter is calculated in the mean-field approach using Skyrme-like parametrizations of the mean-field potentials. In this paper, we simultaneously take into account the LGPT and BEC effects.

The article is organized as follows. In Sec. II A, we formulate main features of the model. The limit of ideal $\alpha - N$ gas is considered in Sec. II B and Appendix A. Pure nucleon and pure α matter with Skyrme interactions are studied in Secs. II C and II D, respectively. The results of these sections are used in choosing parameters of mean fields for $\alpha - N$ matter in Sec. III. The EoS and phase transitions of such matter are studied numerically in Sec. IV. Finally, the conclusions and outlook are given in Sec. V.

II. GENERAL REMARKS AND LIMITING CASES

A. Chemical equilibrium conditions

Let us consider the isosymmetric system (with equal numbers of protons and neutrons) composed of nucleons N and α particles. A small difference between the proton and the neutron masses and the Coulomb interaction effects will be neglected. Our consideration will be restricted to small temperatures $T \lesssim 30$ MeV. In this case, production of pions and other mesons as well as excitation of baryonic resonances, such as Δ and N^*, become negligible. Besides, the masses $m_N \simeq 938.9$ MeV and $m_\alpha \simeq 3727.3$ MeV are much larger than the system temperature, thus, a nonrelativistic approximation can be used in the lowest order in T/m_N.

In the grand canonical ensemble, the pressure $p(T,\mu)$ is a function of temperature T and baryon chemical potential μ. The latter is responsible for conservation of the baryon charge. The chemical potentials of N and α satisfy the relations,

$$\mu_N = \mu, \quad \mu_\alpha = 4\mu, \tag{1}$$

which correspond to the condition of chemical equilibrium in the $N - \alpha$ mixture due to reactions $\alpha \leftrightarrow 4N$. The baryonic number density $n_B(T,\mu) = n_N + 4n_\alpha$, the entropy density $s(T,\mu)$, and the energy density $\varepsilon(T,\mu)$ can be calculated from $p(T,\mu)$ as

$$n_B = \left(\frac{\partial p}{\partial \mu}\right)_T, \quad s = \left(\frac{\partial p}{\partial T}\right)_\mu, \quad \varepsilon = Ts + \mu n_B - p, \tag{2}$$

in the thermodynamic limit where the system volume goes to infinity.

B. Ideal gas limit

Let us first consider the $\alpha - N$ system as a mixture of the ideal Fermi gas of nucleons and the ideal Bose gas of α's. The pressure of such a system is equal to the sum of partial pressures,

$$p^{\rm id}(T,\mu) = p_N^{\rm id}(T,\mu_N) + p_\alpha^{\rm id}(T,\mu_\alpha). \tag{3}$$

Here ($\hbar = c = k_B = 1$),

$$p_i^{\rm id}(T,\mu_i) = \frac{g_i}{(2\pi)^3}\int d^3k \frac{k^2}{3E_i}\left[\exp\left(\frac{E_i - \mu_i}{T}\right) \pm 1\right]^{-1} \quad (i = N, \alpha), \tag{4}$$

where $E_i = \sqrt{m_i^2 + k^2}$ and g_i is the spin-isospin degeneracy factor ($g_\alpha = 1$, $g_N = 4$). Upper and lower signs in Eq. (4) correspond to $i = N$ and $i = \alpha$, respectively.

By taking derivatives with respect to μ_i, one gets the partial densities,

$$n_i = \left(\frac{\partial p_i^{\rm id}}{\partial \mu_i}\right)_T = \frac{g_i}{(2\pi)^3}\int d^3k \left[\exp\left(\frac{E_i - \mu_i}{T}\right) \pm 1\right]^{-1} \quad (i = N, \alpha). \tag{5}$$

In the following, we will also use the canonical variables T, n_i as independent quantities. The transition from the grand canonical variables T, μ_i is performed by solving the transcendental equations (5) with respect to μ_i. Allowable states of the chemically equilibrated $\alpha - N$ mixture are then found using Eq. (1).

The chemical potential of α particles is restricted by the relation $\mu_\alpha \leqslant m_\alpha$. At $\mu_\alpha = m_\alpha$, the Bose condensation of α's occurs. In this case, a nonzero density of Bose-condensed (zero-momentum) α particles n_{bc} should be taken into account. By taking the lowest-order approximation in T/m_i (see the Appendix) and introducing the thermal wavelength of the ith particle $\lambda_i(T) = (2\pi/m_i T)^{1/2}$, one gets the following relations for the total density and pressure of α's in the region of the BEC:

$$n_\alpha = n_\alpha^*(T) + n_{bc}, \quad p_\alpha^{\rm id} = p_\alpha^*(T) \quad (\mu_\alpha = m_\alpha). \tag{6}$$

Here,

$$n_\alpha^*(T) = n_\alpha(T, \mu_\alpha \to m_\alpha - 0) \simeq \frac{g_\alpha}{\lambda_\alpha^3(T)}\zeta(3/2),$$
$$p_\alpha^*(T) \simeq \frac{g_\alpha T}{\lambda_\alpha^3(T)}\zeta(5/2), \tag{7}$$

where $\zeta(x) = \sum_{k=1}^\infty k^{-x}$ is the Riemann ζ function [$\zeta(3/2) \simeq 2.612$, $\zeta(5/2) \simeq 1.341$].

The condition (1) leads to the relations $\mu \equiv \mu_N = \mu_\alpha/4 \leqslant m_\alpha/4 = m_N - B_\alpha$, where $B_\alpha = m_N - m_\alpha/4 \simeq 7.1$ MeV is the binding energy per baryon of the α nucleus. At $\mu = m_N - B_\alpha$, the BEC occurs in the ideal gas. Using Eq. (A1), one obtains the nucleon density in the BEC region,

$$n_N = n_N^*(T) \simeq \frac{g_N}{\lambda_N^3(T)}\Phi_{3/2}^+\left(-\frac{B_\alpha}{T}\right), \tag{8}$$

where $\Phi_{3/2}^+(\eta)$ is a dimensionless function defined in the Appendix. Note that n_N^* does not depend on n_{bc}. From Eqs. (7) and (8), one can get the following relations for the ideal $\alpha - N$ gas in the BEC domain:

$$\frac{n_N}{n_\alpha} \leqslant \frac{n_N^*}{n_\alpha^*} < \frac{1}{2\zeta(3/2)}e^{-B_\alpha/T}. \tag{9}$$

Here, we take into account that $\Phi_{3/2}^+(\eta) < e^\eta$ and $\lambda_\alpha/\lambda_N \simeq 1/2$. According to (9), the fraction of unbound nucleons is small in the whole BEC region, especially at low temperatures (this conclusion has been earlier made in Ref. [24]). Figure 1 shows n_α^*, n_N^* as well as the baryon density of the ideal gas at the BEC boundary as functions of T. One can see that $n_N^* \ll n_\alpha^*$ even at high temperatures.

At each temperature, the chemical equilibrium condition (1) gives a line of allowable states on the (n_N, n_α) plane. These lines are shown in Fig. 2. Vertical sections of the lines correspond to the BEC states with densities $n_N = n_N^*(T)$ and

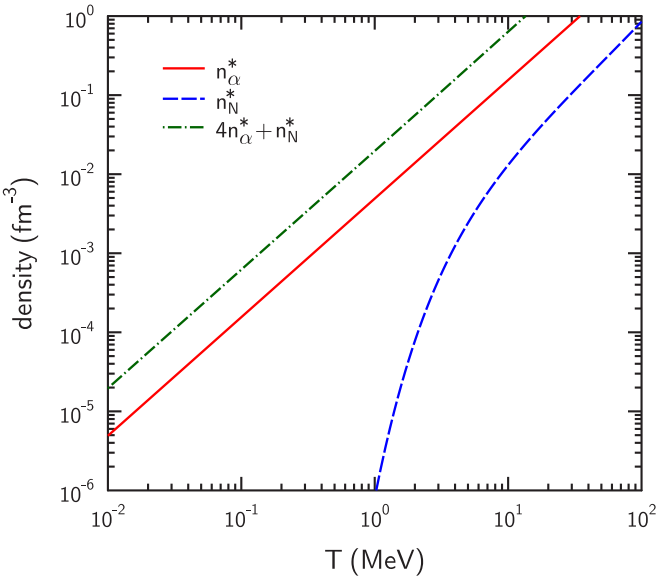

FIG. 1. Densities of α's (the solid line), nucleons (the dashed curve), and the baryon density (the dashed-dotted line) at the BEC boundary as functions of temperature for the ideal $\alpha - N$ gas.

$n_\alpha > n^*_\alpha(T)$. Such states lie above the BEC boundary shown by the thin solid curve in Fig. 2.

C. Pure nucleon matter

Let us consider the limiting case of the one-component isosymmetric nucleon matter with interaction. The EoS and the phase diagram of a pure N matter were studied by many authors. In particular, the mean-field approximation has been applied in Refs. [25–27]. In such an approach, one introduces a shift of the chemical potential μ_N with respect to the ideal nucleon gas. We apply the equation,

$$\widetilde{\mu}_N = \mu_N - U_N(n_N), \tag{10}$$

where $U_N(n_N)$ is the mean-field potential of nucleons and $\widetilde{\mu}_N = \widetilde{\mu}_N(T, n_N)$ is the effective chemical potential of nucleons at the density n_N and temperature T. This quantity is determined by solving Eq. (5) with $i = N$ and $\mu_i = \widetilde{\mu}_N$. Here and below we neglect a possible explicit dependence of the mean-field potential on temperature. Equation (10) leads to the expression,

$$\begin{aligned}\Delta p_N &\equiv p_N(T, \mu_N) - p^{\rm id}_N(T, \widetilde{\mu}_N) \\ &= n_N U_N(n_N) - \int_0^{n_N} dn_1 U_N(n_1)\end{aligned} \tag{11}$$

for the shift of the nucleon pressure with respect to its ideal gas value.[1] One can see that Δp_N does not depend on T. From Eqs. (10) and (11), one can prove the validity of the thermodynamic consistency relation $n_N = (\partial p_N/\partial \mu_N)_T$.

Further on, we use the Skyrme-like parametrization [27] of the mean field,

$$U_N(n_N) = -2a_N n_N + \frac{\gamma+2}{\gamma+1} b_N n_N^{\gamma+1}, \tag{12}$$

where positive constants a_N, b_N, and γ are adjustable parameters. The first and second terms, respectively, describe contributions of medium-range attractive and short-range repulsive interactions of nucleons. Substituting (12) into Eq. (11), one obtains

$$\Delta p_N = -a_N n_N^2 + b_N n_N^{\gamma+2}. \tag{13}$$

Parameters entering Eqs. (12) and (13) are chosen to reproduce phenomenological properties of equilibrium isosymmetric nuclear matter at $T = 0$. We use the values [27],

$$\min\left(\frac{E}{B}\right) = -15.9\,\text{MeV}, \quad n_N = n_0 = 0.15\,\text{fm}^{-3} \quad (T=0) \tag{14}$$

for the binding energy per baryon $E/B = \varepsilon_N/n_N - m_N$ and the saturation density n_0. Using further the thermodynamic identities at zero temperature, $p_N = n_N^2 d(\varepsilon_N/n_N)/dn_N$ and $\mu_N = (\varepsilon_N + p_N)/n_N$, one finds the equations which are equivalent to (14),

$$\mu_N = \mu_0 = 923\ \text{MeV}, \quad p_N = 0 \quad (T = 0,\ n_N = n_0). \tag{15}$$

At $T \to 0$, one can calculate the integrals in Eqs. (4) and (5) for $i = N$ analytically. In this limit, the Fermi distributions inside these integrals can be replaced by unity if $k < k_F$ where $k_F = (6\pi^2 n_N/g_N)^{1/3}$ is the Fermi momentum of nucleons. One gets the relations,

$$\begin{aligned}\widetilde{\mu}_N(T=0, n_N) &= E_F(n_N) = \sqrt{k_F^2 + m_N^2}, \\ p^{\rm id}_N(T=0, n_N) &= \frac{g_N}{6\pi^2}\int_0^{k_F} \frac{k^4 dk}{\sqrt{k^2+m_N^2}}.\end{aligned} \tag{16}$$

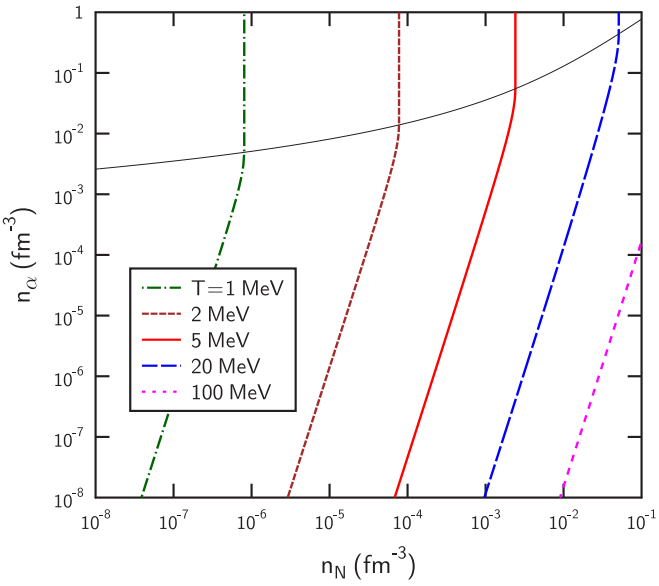

FIG. 2. Isotherms of the chemical equilibrium for an ideal $\alpha - N$ gas. The thin solid line shows the boundary of the BEC region.

[1]This shift is often called the "excess" pressure [25,26].

TABLE I. Characteristics of pure nucleon matter in the Skyrme mean-field model.

γ	a_N (GeV fm^3)	b_N (GeV fm$^{3+3\gamma}$)	K_N (MeV)	T_c (MeV)	n_c (fm^{-3})	$\mu_c - m_N$ (MeV)
1/6	1.167	1.475	198	15.3	0.048	−31.6
1	0.399	2.049	372	21.3	0.059	−42.8

From Eqs. (10), (11), (15), and (16) one obtains two equations,

$$U_N(n_0) = \mu_0 - E_F(n_0),$$
$$\Delta p_N(n_0) = -p_N^{\rm id}(T=0, n_0) \tag{17}$$

for the parameters a_N, b_N as functions of γ.

The results of the numerical calculation for $\gamma = 1/6$ and $\gamma = 1$ are shown in Table I. In addition to coefficients of the Skyrme interactions, we also present the values of the incompressibility modulus,

$$K_N = 9\frac{dp_N}{dn_N} = 9n_N\frac{d(E_F + U_N)}{dn_N}, \tag{18}$$

at the saturation point $n_N = n_0,\ T = 0$. As noted in Ref. [28], the Skyrme-like models with $1/6 \leqslant \gamma \leqslant 1/3$ predict reasonable values of the nuclear matter compressibility $K_N = 200 - 240$ MeV.[2] This agrees with our calculations. Indeed, one can see from Table I that the "soft" Skyrme parametrization with $\gamma = 1/6$ is preferable as compared to $\gamma = 1$.

Using Eqs. (2), (4), (5), and (10)–(13) one can calculate all thermodynamic functions of pure nucleon matter at nonzero temperatures. Our mean-field model predicts a first-order LGPT at temperatures $0 \leqslant T \leqslant T_c$, where T_c is the critical temperature. Characteristics of the LGPT are found by using Gibbs conditions of the phase equilibrium [30]. For isotherms with $T < T_c$, there are two (meta)stable branches of the chemical potential as the function of pressure. In accordance with Gibbs rule, these branches intersect at the LGPT point. We find the intersection points numerically by calculating isotherms on the chemical potential-pressure plane. The position of the critical point is found by solving two equations [30]: $(\partial\, p_N/\partial n_N)_T = 0,\ (\partial^2 p_N/\partial n_N^2)_T = 0$. The characteristics of this point for the soft ($\gamma = 1/6$) and stiff ($\gamma = 1$) repulsive interactions are given in the last three columns of Table I.

Figures 3(a) and 3(b) show the phase diagrams of nucleonic matter on the (μ, T) and (n_B, T) planes, respectively. The LGPT line in Fig. 3(a) goes from the ground state (GS) at $T = 0,\ \mu = \mu_0$ to the critical point at $T = T_c,\ \mu = \mu_c$. According to our calculations, T_c increases, but μ_c decreases with γ. Figure 3(b) shows the "binodals," i.e., the boundaries of the liquid-gas mixed phase (MP). They intersect the density axis at $n_B = n_N = n_0$.

[2]See, however, Ref. [29] where higher values of $K_N = 250$–315 MeV have been obtained from the fit of data on the giant monopole resonance.

D. Pure α matter

In this section, we consider the idealized case of a pure α matter. In this limit, reactions $\alpha \leftrightarrow 4N$ are disregarded and, therefore, the chemical equilibrium is violated. Up to now, the EoS of such matter has been poorly known. The variational microscopic calculations based on phenomenological $\alpha\alpha$ potentials were performed a long time ago in Ref. [7]. More recently, the EoS of pure α matter was considered within several simplified models in Refs. [10,11]. In Ref. [6], the phase diagram of such matter has been studied within a Skyrme mean-field model. Below, we apply the same approach and use characteristics of the α-matter GS obtained in Ref. [7],

$$W_\alpha = -\min\left(\frac{E_\alpha}{B}\right) = 12\ \text{MeV},$$
$$n_\alpha = n_{0\alpha} = 0.036\ \text{fm}^{-3} \quad (T = 0). \tag{19}$$

Note that the baryon density of this state $4n_{0\alpha} \simeq 0.144$ fm^{-3} is close to the saturation density of pure nucleon matter, but the latter has stronger binding per baryon [compare Eqs. (14) and (19)].

In the case of pure α matter, one can write the equations, analogous to Eqs. (10)–(13),

$$\widetilde{\mu}_\alpha = 4\mu - U_\alpha(n_\alpha), \quad p_\alpha = p_\alpha^{\rm id}(T, \widetilde{\mu}_\alpha) + \Delta p_\alpha(n_\alpha), \tag{20}$$

where μ is the baryon chemical potential and U_α and Δp_α are parameterized by Eqs. (12) and (13) with the replacement $N \to \alpha$. Below, we choose the same parameter γ as for nucleons and find the coefficients a_α and b_α from the conditions (19).

In our mean-field model, one has the following relations for states with the BEC of α particles:

$$\widetilde{\mu}_\alpha = m_\alpha, \quad n_\alpha \geqslant n_\alpha^*(T), \quad p_\alpha^{\rm id} = p_\alpha^*(T), \tag{21}$$

where n_α^* and p_α^* are defined in Eq. (7). The boundary of the BEC region is obtained after replacing the inequality in (21) by the equality. The resulting equation $4\mu = m_\alpha + U_\alpha[n_\alpha^*(T)]$ gives a line on the (μ, T) plane. For brevity, we call it the BEC line.

At zero temperature one has $n_\alpha^* = 0$ and $p_\alpha^* = 0$ and the conditions (21) hold for all states. In this case, Eqs. (20) give

$$4\mu = m_\alpha + U_\alpha(n_\alpha), \quad p_\alpha = \Delta p_\alpha(n_\alpha) \quad (T = 0). \tag{22}$$

Using further the relations $E_\alpha/B = \varepsilon_\alpha/4n_\alpha - m_N$ and $p_\alpha = 4\mu n_\alpha - \varepsilon_\alpha = 0$ for the GS of α matter, one gets algebraic equations for the coefficients of the Skyrme interaction [6],

$$U_\alpha(n_{0\alpha}) = 4(B_\alpha - W_\alpha), \quad \Delta p_\alpha(n_{0\alpha}) = 0, \tag{23}$$

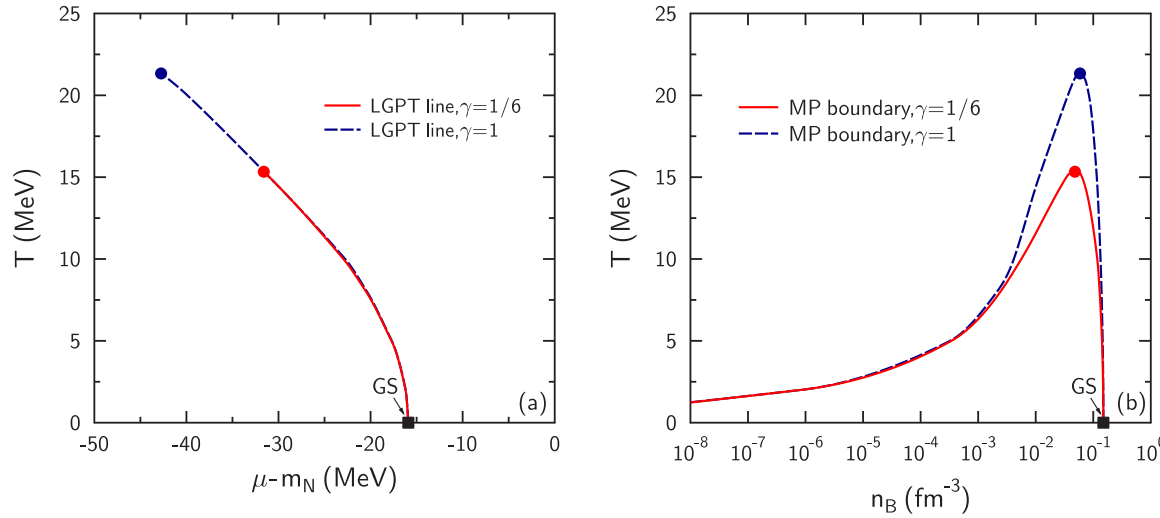

FIG. 3. Phase diagrams of isosymmetric nucleon matter on (a) the (μ, T) and (b) the (n_B, T) planes. The solid and dashed lines correspond to the LGPT at $\gamma = 1/6$ and $\gamma = 1$, respectively. Full dots mark the positions of the critical points (CPs). The ground state is shown by the full square.

where B_α was introduced in Sec. II B. The solutions of Eqs. (23) can be written as

$$a_\alpha = b_\alpha n_{0\alpha}^\gamma = \frac{4(\gamma+1)}{\gamma n_{0\alpha}}(W_\alpha - B_\alpha). \tag{24}$$

Numerical values of the coefficients a_α and b_α as well as the compressibility $K_\alpha = 9\gamma a_\alpha n_{0\alpha}$ are given in Table II for the soft and stiff Skyrme repulsions.

Using the Skyrme interaction, one can calculate the thermodynamical functions of pure α matter at nonzero temperatures. Similar to the pure nucleon matter, the model predicts the LGPT in a pure α system. On the (μ, T) plane, this phase transition occurs along a line which goes from the GS at $T = 0$ to the critical point at $T = T_c$, $\mu = \mu_c$. The presence of the BEC imposes some complications as compared to the case of pure nucleon matter. We found that the BEC boundary crosses the LGPT line at some "triple" point with temperature $T_{\rm TP} < T_c$.

The resulting phase diagrams on the (μ, T) and (n_B, T) planes are shown in Figs. 4(a) and 4(b), respectively (note that $n_B = 4n_\alpha$ for pure α matter). The characteristics of the CP as well as the temperature of the triple point are given in Table II. Similar to pure nucleon matter, the value of $T_c(\mu_c)$ increases (decreases) with γ, but the position of the triple point only slightly depends on this parameter. Note that the BEC region in Fig. 4(a) extends to the right from the LGPT line and below the BEC line. According to Fig. 4(b), the BEC line on the (n_B, T) plane is not sensitive to γ outside the MP region. It is clear that inside this region the BEC occurs only in the liquid phase, whose volume fraction diminishes with decreasing n_B. Therefore, the volume fraction of the condensate decreases too and vanishes at the left binodal boundary. The horizontal lines in Fig. 4(b) show the BEC critical temperatures in the MP domain for two considered values of γ.

III. SKYRME MODEL FOR $\alpha - N$ BINARY MIXTURE

A. Thermodynamic relations for the two-component system

Similar to one-component matter, we take into account multiparticle interactions in the $\alpha - N$ mixture by introducing a temperature-independent excess part of pressure Δp,

$$p = p_N^{\rm id}(T, n_N) + p_\alpha^{\rm id}(T, n_\alpha) + \Delta p(n_N, n_\alpha). \tag{25}$$

A similar expression can be written for the free-energy density $f = \sum_{i=N,\alpha} \mu_i n_i - p$ after introducing the excess term $\Delta f = f - f_N^{\rm id} - f_\alpha^{\rm id}$. At known Δp, one can calculate the mean-field potentials $U_i = \mu_i - \widetilde{\mu}_i$ as well as the excess free-energy Δf. The following relations can be obtained [31,32]:

$$\begin{aligned} U_N(n_N, n_\alpha) &= \left(\frac{\partial\, \Delta f}{\partial n_N}\right)_{n_\alpha}, \\ U_\alpha(n_N, n_\alpha) &= \left(\frac{\partial\, \Delta f}{\partial n_\alpha}\right)_{n_N}, \\ \Delta f(n_N, n_\alpha) &= \int_0^1 \frac{d\lambda}{\lambda^2} \Delta p(\lambda n_N, \lambda n_\alpha). \end{aligned} \tag{26}$$

TABLE II. Characteristics of pure α matter in the Skyrme model.

γ	a_α (GeV fm^3)	b_α (GeV fm$^{3+3\gamma}$)	K_α(MeV)	T_c (MeV)	n_{Bc} (fm^{-3})	$\mu_c - m_N$ (MeV)	$T_{\rm TP}$ (MeV)
1/6	3.831	6.667	207	10.2	0.037	−16.7	3.56
1	1.094	30.39	354	13.7	0.048	−19.3	3.65

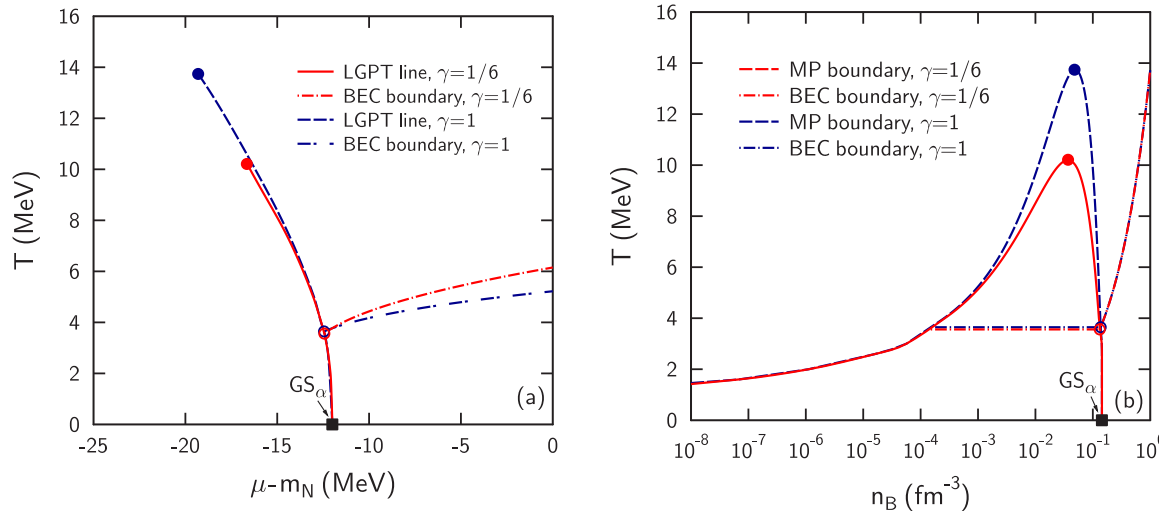

FIG. 4. Phase diagrams of pure α matter on the (a) (μ, T) and (b) (n_B, T) planes. The solid and dashed curves correspond to $\gamma = 1/6$ and $\gamma = 1$, respectively. The full dots mark the positions of the CPs. The GS of the α matter is shown by the full square. The dashed-dotted lines represent the boundaries of the BEC regions. The open dots show the positions of the triple points. They practically coincide for two considered values of γ.

In addition, one can find the entropy density $s = -\partial f/\partial T = \sum_i s_i^{\rm id}$ and the energy density $\varepsilon = f + Ts = \sum_i \varepsilon_i^{\rm id} + \Delta f$, where $s_i^{\rm id}$ and $\varepsilon_i^{\rm id}$ are the corresponding ideal-gas quantities for ith species $(i = N, \alpha)$.

The free-energy density is a genuine thermodynamic potential in the canonical ensemble. Instead of partial densities n_N and n_α, one can also use the variables,

$$n_B = n_N + 4n_\alpha, \quad \chi = \frac{4n_\alpha}{n_B}. \tag{27}$$

The quantity χ is a fraction of bound nucleons in the $\alpha - N$ matter (it is approximately equal to the mass fraction of α's). Note that, due to the baryon number conservation $B = N_N + 4N_\alpha = \text{const}$, the baryon density n_B is inversely proportional to the system volume V. Using Eq. (27) and thermodynamic identities, one can write the following relations for changes in the free-energy per baryon in any isothermal process:

$$d\left(\frac{F}{B}\right) = d\left(\frac{f}{n_B}\right) = p\frac{dn_B}{n_B^2} + \left(\frac{\mu_\alpha}{4} - \mu_N\right)d\chi \quad (T = \text{const}). \tag{28}$$

According to this equation, at fixed T and n_B, the quantity F/B reaches its extremum if the condition (1) is satisfied. However, solving Eq. (1) with respect to χ does not necessarily gives the true state of the chemical equilibrium. In particular, the solution can be unstable $(F/B = \max)$ if the second derivative of F/B over χ is negative.

In general, one should explicitly calculate the curvature matrix $(\partial^2 f/\partial n_i \partial n_j)_T$ to study stability of the system with respect to fluctuations of partial densities n_N, n_α. Only if both eigenvalues of this matrix are non-negative, will the corresponding state be stable.[3] The necessary condition of stability can be written as [33]

$$\det\left(\frac{\partial^2 f}{\partial n_i \partial n_j}\right)_T = \det\left(\frac{\partial \mu_i}{\partial n_j}\right)_T = \left(\frac{\partial \mu_N}{\partial n_N}\right)_T \left(\frac{\partial \mu_\alpha}{\partial n_\alpha}\right)_T - \left(\frac{\partial \mu_N}{\partial n_\alpha}\right)_T^2 \geqslant 0. \tag{29}$$

B. Skyrme parametrization of interaction terms

In the present paper, we apply a generalized Skyrme-like parametrization for the excess pressure Δp,

$$\Delta p(n_N, n_\alpha) = -\sum_{i,j} a_{ij} n_i n_j + \left(\sum_i B_i n_i\right)^{\gamma+2}, \tag{30}$$

where a_{ij}, B_i, and γ are positive constants and the sums go over $i, j = N, \alpha$. The first term on the right-hand side of Eq. (30) describes attractive forces and has the same structure as in the two-component van der Waals equation of state [16]. The second term, responsible for repulsive interactions, is obtained by interpolation between the limits $n_\alpha = 0$ and $n_N = 0$ considered in Secs. II C and II D. From the comparison with these limiting cases, one gets the relations $a_{ii} = a_i$, $B_i^{\gamma+2} = b_i$ where a_i and b_i are the Skyrme coefficients introduced earlier for the pure nucleon $(i = N)$ and pure α $(i = \alpha)$ matter. Using these relations, one finds

$$\Delta p(n_N, n_\alpha) = -\left(a_N n_N^2 + 2a_{N\alpha} n_N n_\alpha + a_\alpha n_\alpha^2\right) + b_N(n_N + \xi n_\alpha)^{\gamma+2}, \tag{31}$$

[3]Note that the appearance of negative-curvature (spinodal) parts of the free-energy density surface can be considered as a necessary condition for the LGPT.

where

$$\xi = \left(\frac{b_\alpha}{b_N}\right)^{1/(\gamma+2)} = \begin{cases} 2.006, & \gamma = 1/6, \\ 2.457, & \gamma = 1. \end{cases} \quad (32)$$

Numerical values of ξ in Eq. (32) are obtained by substituting the b_N and b_α values from Tables I and II. One can see that there is only one unknown coefficient in the parametrization (31), namely, the cross-term coefficient $a_{N\alpha}$ which determines the $\alpha - N$ attraction strength. Below, we study the sensitivity to the choice of this parameter.

Using Eqs. (26) and (31), one gets the relations,

$$\Delta f = -\left(a_N n_N^2 + 2a_{N\alpha} n_N n_\alpha + a_\alpha n_\alpha^2\right) + \frac{b_N}{\gamma+1}(n_N + \xi n_\alpha)^{\gamma+2}, \quad (33)$$

$$\mu_N = \widetilde{\mu}_N - 2(a_N n_N + a_{N\alpha} n_\alpha) + \frac{\gamma+2}{\gamma+1} b_N (n_N + \xi n_\alpha)^{\gamma+1}, \quad (34)$$

$$\mu_\alpha = \widetilde{\mu}_\alpha - 2(a_{N\alpha} n_N + a_\alpha n_\alpha) + \frac{\gamma+2}{\gamma+1} b_N \xi (n_N + \xi n_\alpha)^{\gamma+1}. \quad (35)$$

To study the EoS of interacting $\alpha - N$ matter, we choose a certain value of $a_{N\alpha}$ and substitute (34) and (35) into the condition of chemical equilibrium (1). The resulting equation gives allowable states in the (T, n_N, n_α) space. Then, from Eqs. (25), (31), and (34), we determine pressure at different $\mu = \mu_N$'s and T's.

Before going to numerical results we would like to note that our approach becomes questionable at high densities of α particles. Classical Monte Carlo calculations in the hard-sphere approximation show [34] that the transition to a solid phase occurs in a pure α system at $n_\alpha \gtrsim (0.07 - 0.1)$ fm^{-3} (in this estimate, we assume the radius of the α nucleus $r_\alpha = 1 - 1.2$ fm). Therefore, our results should be considered with caution at baryon densities $n_B \gtrsim 0.3 - 0.4$ fm^{-3}.

IV. RESULTS FOR INTERACTING $\alpha - N$ MATTER

A. Zero-temperature limit

Let us consider first the ground state of the $\alpha - N$ matter at zero temperature. Note that this is the state with $p = 0$ and minimal energy per baryon ε/n_B. Using formulas of the preceding section, one can calculate the pressure p, the baryon chemical potential,

$$\mu = \mu_N = \mu_\alpha/4, \quad (36)$$

and the energy per baryon $\varepsilon/n_B = \mu - p/n_B$ at $T \to 0$ as functions of n_B for different values of the parameter $a_{N\alpha}$.

Our analysis shows that the results are qualitatively different if this parameter is smaller or larger than some threshold value a_* [see below Eq. (41)]. In the region $a_{N\alpha} < a_*$ the GS of the $\alpha - N$ mixture corresponds to pure nucleon matter ($n_\alpha = 0$) with $\mu = \mu_0$ and $n_N = n_0$. Here, μ_0 and n_0, respectively, are the chemical potential and the saturation density of the equilibrium nucleon matter, introduced in Sec. II C. In the same interval of $a_{\alpha N}$, there exists another local minimum of energy per baryon with $n_N = 0$ which corresponds to pure α matter. This state is metastable because it has a smaller binding energy as compared to pure nucleon matter. These two minima on the (n_B, χ) plane are separated by an energetic barrier.

Our calculations show that at $a_{N\alpha} > a_*$ the $\alpha - N$ mixture has only one minimum-energy state on the (n_B, χ) plane, and this system becomes stronger bound as compared to pure nucleon matter. In this region, the GS is characterized by a nonzero value of n_α, and the corresponding binding energy $W = m_N - \varepsilon/n_B = m_N - \mu$ increases with $a_{N\alpha}$.

The threshold value a_* can be found analytically by using formulas of the preceding section. One should take into

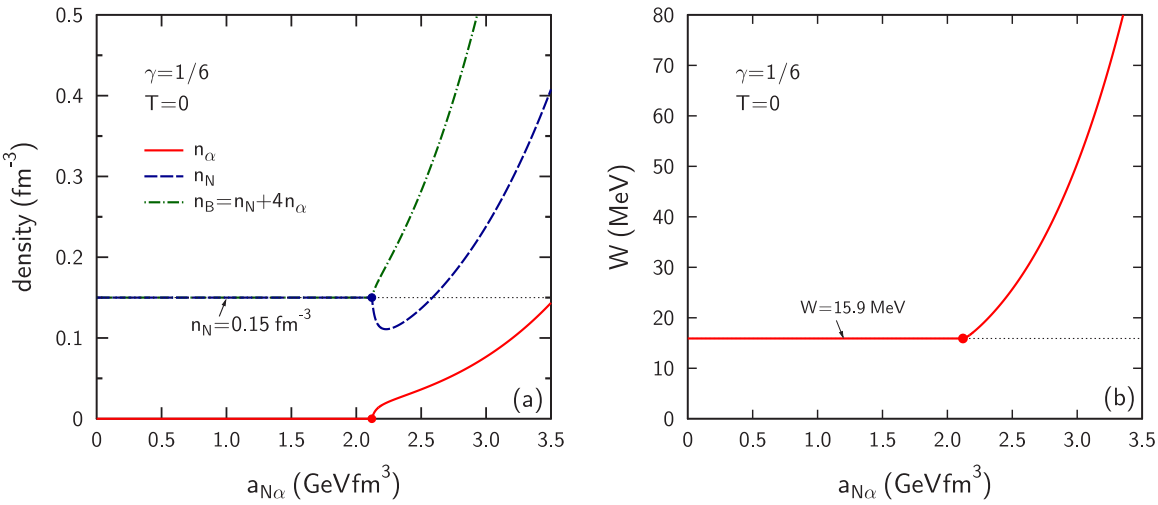

FIG. 5. (a) Partial densities as well as baryon density of particles in the GS of cold $\alpha - N$ matter as functions of the cross-term coefficient $a_{N\alpha}$. (b) Binding energy per baryon of the cold $\alpha - N$ mixture as the function of $a_{N\alpha}$. The dots correspond to threshold value $a_{N\alpha} = a_*$ (see the text). All calculations correspond to $\gamma = 1/6$.

TABLE III. Characteristics of the LGPT for $\alpha - N$ matter at $T = 2$ MeV (set B).

		Binodal point C				Binodal point D			
	$\mu_c - m_N$ (MeV)	n_N (fm^{-3})	n_α (fm^{-3})	n_B (fm^{-3})	χ	n_N (fm^{-3})	n_α (fm^{-3})	n_B (fm^{-3})	χ
PT$_1$	−16.2	8.2×10^{-7}	6.3×10^{-11}	8.2×10^{-7}	3.1×10^{-4}	0.15	2.1×10^{-17}	0.15	1.4×10^{-16}
PT$_2$	−12.1	6.4×10^{-6}	2.3×10^{-7}	7.3×10^{-6}	0.12	7.3×10^{-4}	3.5×10^{-2}	0.14	1.0

account that at zero temperature all α's are Bose condensed ($\widetilde{\mu}_\alpha = m_\alpha$) and the ideal-gas pressure $p_\alpha^{\rm id} = 0$. Using these relations and formulas of Sec. III, one gets the equations,

$$p = p_N^{\rm id} + \Delta p(n_N, n_\alpha) = 0, \tag{37}$$

$$\mu_N = E_F(n_N) + U_N(n_N, n_\alpha), \tag{38}$$

$$\mu_\alpha = m_\alpha + U_\alpha(n_N, n_\alpha), \tag{39}$$

where Δp, U_N, and U_α are functions of n_N, n_α defined in Eqs. (31), (34), and (35).

The ground-state values of μ, n_B, and χ are determined by simultaneously solving Eqs. (36)–(39). They are continuous functions of $a_{N\alpha}$ so that $\mu \to \mu_0$, $n_N \to n_0$, $n_\alpha \to 0$ at $a_{N\alpha} \to a_*$. Substituting these limiting values into (36) and (39) gives

$$m_\alpha + U_\alpha(n_0, 0) = 4\mu_0 \quad (a_{N\alpha} = a_*). \tag{40}$$

Solving this equation with respect to a_* gives

$$a_* = \frac{1}{2}\left(\frac{m_\alpha - 4\mu_0}{n_0} + \frac{\gamma+2}{\gamma+1} b_N \xi\, n_0^\gamma\right)$$
$$\simeq 2.12 \text{ GeV fm}^3 \quad (\gamma = 1/6). \tag{41}$$

In the last equality, we use numerical values of b_N, ξ obtained in Secs. II C and III B.

Figures 5(a) and 5(b) show ground-state characteristics of cold $\alpha - N$ matter as functions of $a_{N\alpha}$ for $\gamma = 1/6$. One can see that at $a_{N\alpha} > a_*$ the binding energy and densities n_α, n_B increase monotonically with $a_{N\alpha}$.

Below, we present the results for $\gamma = 1/6$ and choose the parameter $a_{N\alpha}$ in the interval $a_{N\alpha} < a_*$, i.e., we assume that α's do not appear in the GS at $T \to 0$. Such an assumption seems to be supported by the nuclear phenomenology. To study the sensitivity to $a_{N\alpha}$, we compare the results for $a_{N\alpha} =$ 1 (set A) and 1.9 (set B) GeV fm^3.

B. Phase diagram of interacting $\alpha - N$ matter

In this section, we consider the EoS of chemically equilibrated $\alpha - N$ mixture at nonzero temperatures. We apply explicit relations for pressure and free energy derived in Sec. III B. By solving Eq. (1), one can find allowable states of matter in the (T, μ, p) or (T, n_N, n_α) space. The stability of such states is studied by calculating the sign of the determinant in Eq. (29).

Figure 6 represents the isotherm $T = 2$ MeV on the plane (μ, p). Lower and upper panels correspond to sets A and B, respectively. The unstable parts of the isotherm are shown by the dotted lines. It is interesting that only these parts exhibit significant changes in the transition between sets A and B. According to Gibbs rule, the intersection points of (meta)stable branches of pressure as functions of μ correspond to PTs. As one can see from Fig. 6, there are two PTs at $T = 2$ MeV. Their characteristics, in particular, critical values of the baryon chemical potential μ_c are given in Table III.

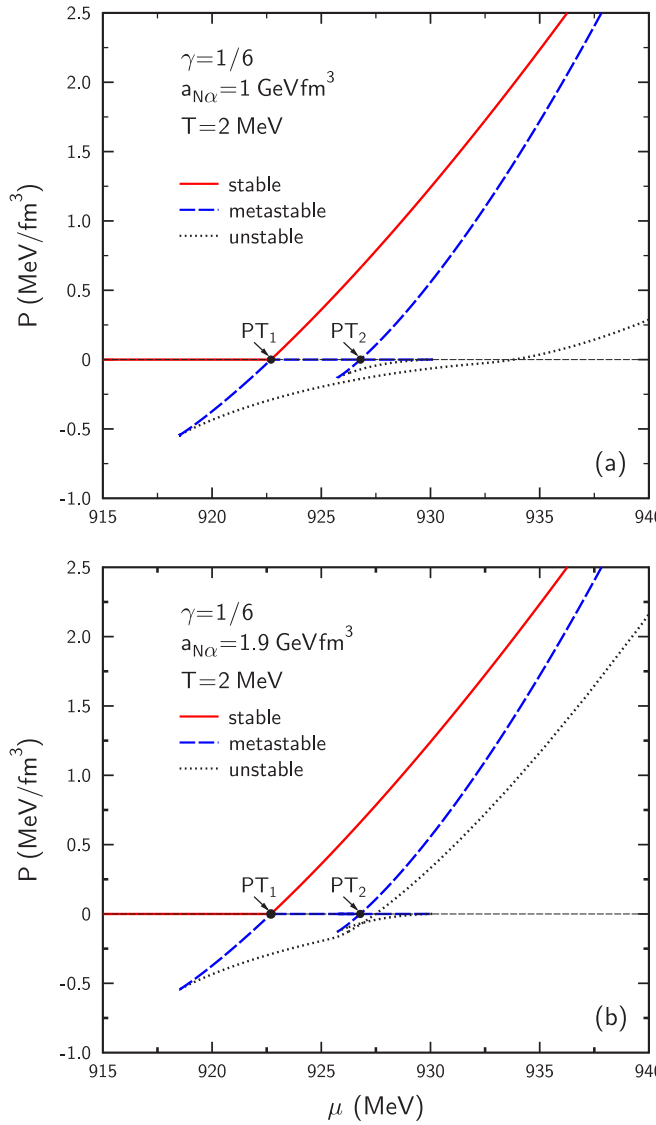

FIG. 6. The isotherm $T = 2$ MeV of $\alpha - N$ matter on the (μ, p) plane for the parameter sets (a) A and (b) B. The stable, metastable, and unstable parts of isotherm are shown by the solid, dashed, and dotted lines, respectively. The dots PT$_1$ and PT$_2$ show positions of stable and metastable LGPTs, respectively.

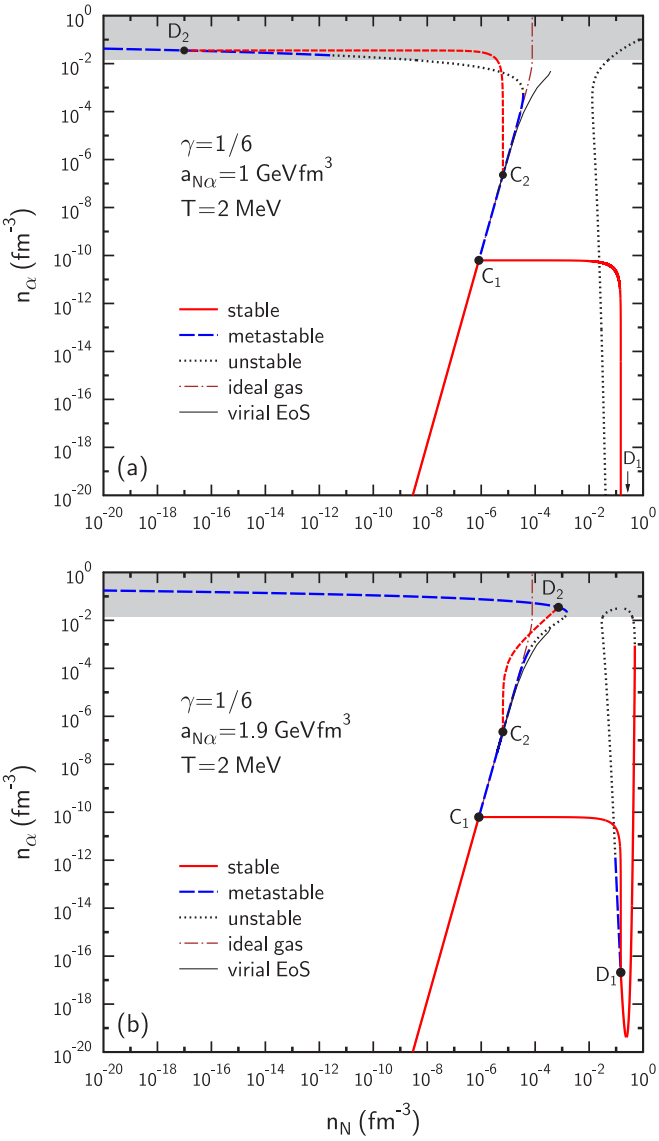

FIG. 7. The isotherm $T = 2$ MeV on the (n_N, n_α) plane for the same parameters as in Fig. 6. The BEC region is shown by shading. The dashed-dotted line corresponds to ideal $\alpha - N$ gas. Lines C_1D_1 and C_2D_2 correspond to mixed-phase states of PT_1 and PT_2, respectively. The thin solid line represents the isotherm $T = 2$ MeV from Ref. [15]. Note that the binodal point D_1 in the upper panel lies below the plotted region.

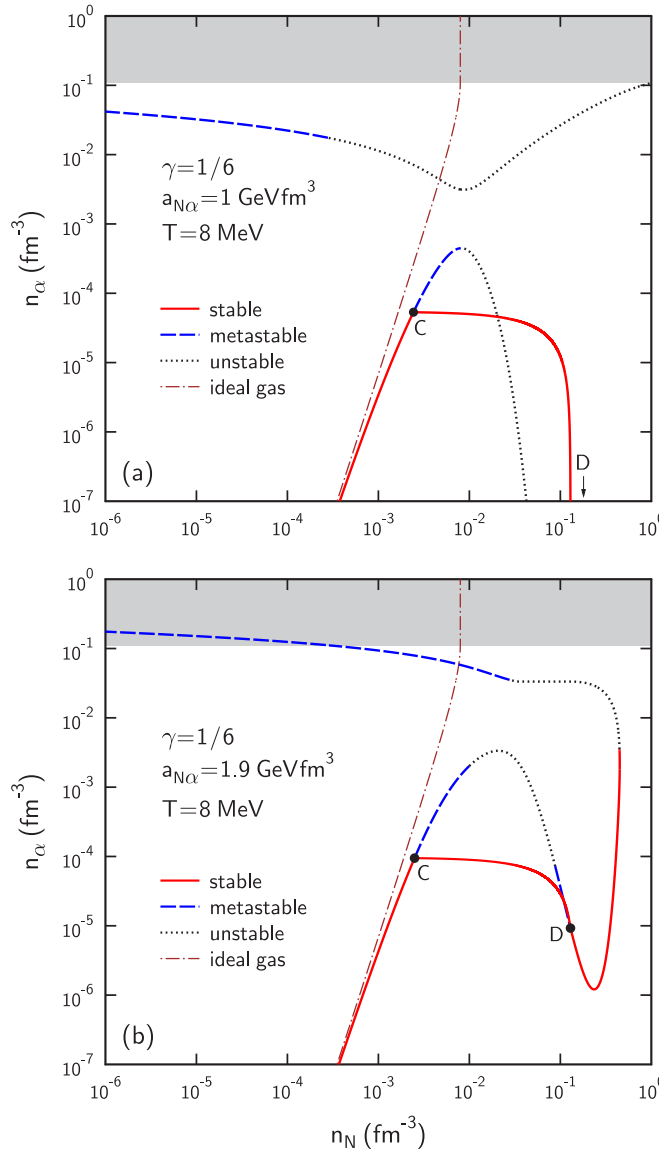

FIG. 8. The same as Fig. 7 but for $T = 8$ MeV. Note that only one (stable) LGPT exists at this temperature.

The first transition PT_1 occurs at a smaller baryon chemical potential as compared to PT_2.[4] As a consequence, states on the dashed lines have lower pressure (i.e., larger thermodynamic potential $\Omega = -pV$) as compared to states with the same μ on the solid curve. It is well known that states with lower pressure are thermodynamically less favorable [30,35]. This shows that states on the dashed lines (including mixed-phase states of PT_2) are metastable. In Figs. 6–8 stable (favorable) states are represented by the solid lines, and metastable (unfavorable) states are indicated by the dashed lines. The unstable states with maximum values of Ω are shown by the dotted lines.

Figures 7(a) and 7(b) represent the same isotherm $T = 2$ MeV, but on the (n_N, n_α) plane. A strong sensitivity to $a_{N\alpha}$ is clearly visible in this representation. By shading, we show the region of BEC $n_\alpha > n_\alpha^* \simeq 0.014$ fm^{-3} (see Sec. II B). For both sets of parameters, we do not find any stable states of the $\alpha - N$ matter with large fractions of α's at densities $n_N \gtrsim 10^{-2}$ fm^{-3}. One may say that the model imitates the Mott effect [36], i.e., predicts a suppression of nuclear clusters at large baryon densities. On the other hand, the model also predicts metastable states, where α particles are more abundant than nucleons (see, e.g., the upper parts of Figs. 7 and 8 where the dashed lines enter the shaded area).

Points C_i and D_i in Fig. 7 and Table III are the binodal points (i.e., the boundaries of the liquid-gas MP) for the phase

[4]Note that the slope of the pressure as a function of μ equals the baryon density n_B. Therefore, jumps in the pressure slopes at points PT_1 and PT_2 in Fig. 6 correspond to nonzero jumps in n_B.

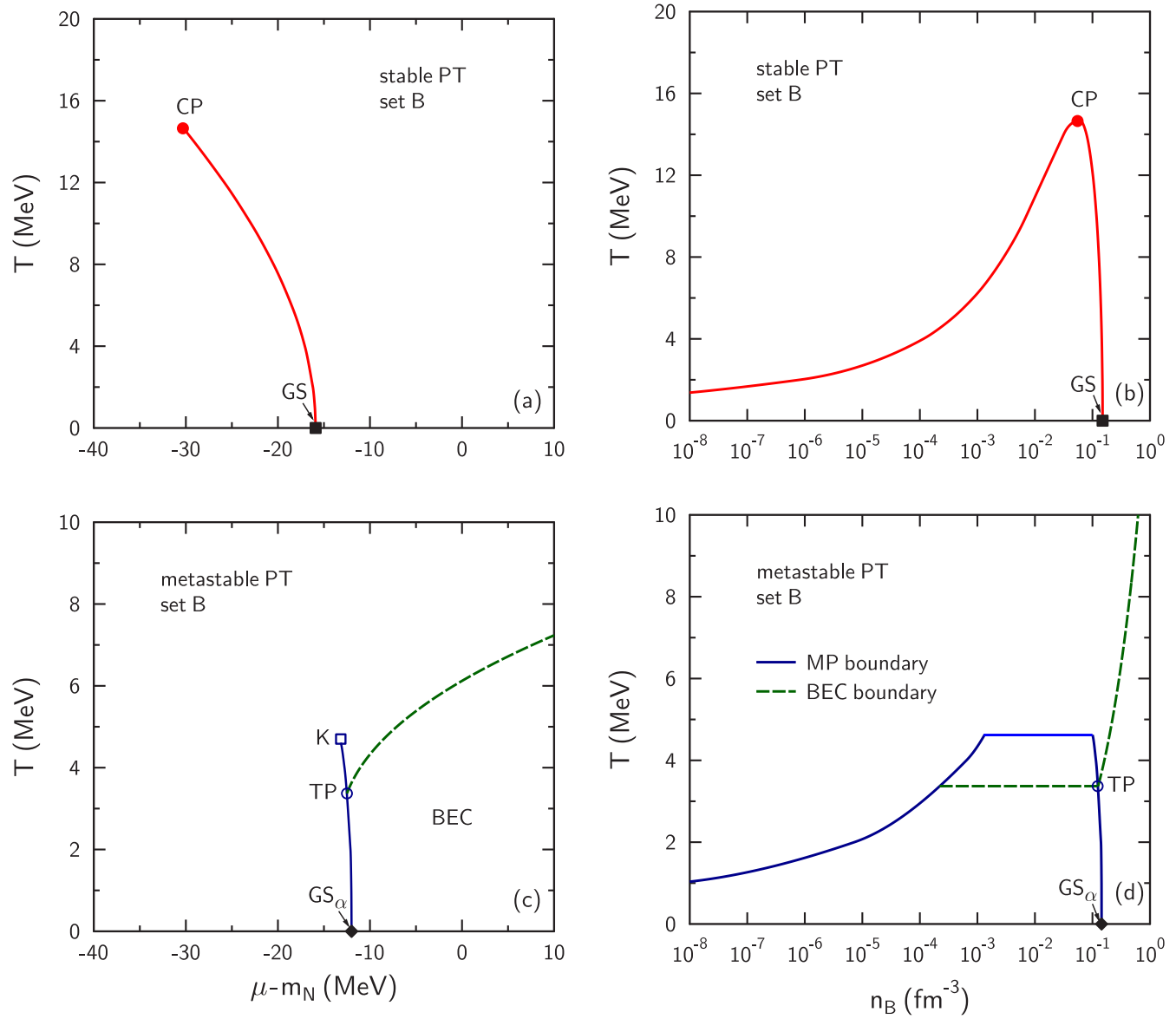

FIG. 9. Left panels: critical lines of (a) the stable and (c) the metastable PTs of $\alpha - N$ matter on the (μ, T) plane. Right panels: boundaries of MP for (b) the stable and (d) the metastable PTs of the $\alpha - N$ mixture on the (n_B, T) plane. All calculations correspond to parameter set B. The full circles in (a) and (b) show the positions of the CPs. The dashed lines in (c) and (d) represent boundaries of the BEC region. The open square (circle) marks the end (triple) point of the metastable PT. The full squares and diamonds show the GS positions for the pure nucleon and pure α matter, respectively.

transition PT$_i$ $(i = 1, 2)$. Coordinates of such points on the (n_N, n_α) plane are determined from Gibbs conditions of phase equilibrium,

$$p\left(T, n_N^{(C)}, n_\alpha^{(C)}\right) = p\left(T, n_N^{(D)}, n_\alpha^{(D)}\right) = p_c, \tag{42}$$

$$\mu_N\left(T, n_N^{(C)}, n_\alpha^{(C)}\right) = \mu_N\left(T, n_N^{(D)}, n_\alpha^{(D)}\right) = \mu_c, \tag{43}$$

where we omit indices i. Characteristics of binodal points for the parameter set B are given in Table III.[5] We have checked that at $T = 2$ MeV the nucleon densities at points C_1 and D_1 are close to the binodal densities of pure nucleon matter (see Sec. II C). The same conclusion is valid for the α-particle densities at points C_2 and D_2: They are close to the binodal densities obtained for pure α matter in Sec. II D. Note that for both parameter sets point D_2 lies in the BEC region.

The solid and short-dashed lines C_1D_1 and C_2D_2 in Fig. 7 correspond to the MP states for PT$_1$ and PT$_2$, respectively. Coordinates of these states on the (n_N, n_α) plane and the volume fraction of the liquid phase λ satisfy the relations (as above, we omit the phase transition index),

$$\lambda = \frac{n_N - n_N^{(C)}}{n_N^{(D)} - n_N^{(C)}} = \frac{n_\alpha - n_\alpha^{(C)}}{n_\alpha^{(D)} - n_\alpha^{(C)}}. \tag{44}$$

[5]The calculation with set A gives a very small value (about 10^{-74} fm^{-3}) for the α-particle density at the binodal point D_1. The latter lies far below the horizontal axis in Fig. 7(a).

TABLE IV. Characteristics of phase transitions in $\alpha - N$ matter for parameter sets A and B.

	PT_1				PT_2				
	T_{CP} (MeV)	$\mu_{CP} - m_N$ (MeV)	n_{BCP} (fm^{-3})	χ_{CP}	T_K (MeV)	$\mu_K - m_N$ (MeV)	n_{BK} (fm^{-3})	χ_K	T_{TP} (MeV)
Set A	15.4	−31.7	4.8×10^{-2}	2.5×10^{-4}	7.6	−14.3	$(1.2 - 2.6) \times 10^{-2}$	0.14–1.0	3.54
Set B	14.7	−30.3	5.3×10^{-2}	6.9×10^{-2}	4.6	−13.2	1.3×10^{-3}–10^{-1}	0.46–0.86	3.37

One can see that the MP states lie on straight lines on the (n_N, n_α) plane. However, one can hardly recognize this linear dependence in Fig. 7 because of the double-logarithmic scale used in this plot.

As one can see from Table III and Fig. 7, the mass fraction of α's χ is relatively small for the MP states of PT_1, but it is rather large for the transition PT_2. As has been already mentioned, the phase transition PT_2 is, in fact, metastable. Nevertheless, we believe that it can be observed in dynamical processes (such as heavy-ion collisions) by selecting states with large relative abundances of α's. The same statement can be made for BEC states (see the dashed lines in the shaded regions). Indications of an enhanced production of α's and α-conjugate nuclei have been observed recently in intermediate-energy nuclear collisions [37,38].

The results obtained within a virial approach [15] are shown in Fig. 7 by thin solid lines. This approximation can be considered as reasonable only at low densities. Note that the quantum-statistical and phase-transition effects are disregarded in such a model. Nevertheless, from Fig. 7 one can conclude that calculations with set B are in better agreement with the results of Ref. [15]. Presumably, this parameter set is preferable as compared to set A.

Figures 8(a) and 8(b) show the isotherm $T = 8$ MeV on the (n_N, n_α) plane again for the parameter sets A and B. At this temperature only one stable LGPT remains. One can see a significant change in the shape of the isotherm as compared to the case $T = 2$ MeV considered in Fig. 7.

A further increase in T leads to the disappearance of the LGPT. This takes place at $T > T_{CP}$ where T_{CP} is the temperature of the CP. Similar to the pure nucleon and α matter, we determine the characteristics of this point by simultaneously solving the equations $(\partial p/\partial n_B)_T = 0$ and $(\partial^2 p/\partial n_B^2)_T = 0$. Our analysis shows that the metastable transition PT_2 disappears "abruptly" at some temperature, T_K, which is smaller than T_{CP}. Note that there is still a nonzero baryon density jump at $T = T_K$ [see Fig. 9(d)].[6]

Table IV gives the characteristics of the critical point of PT_1 as well as those for the end point K of PT_2. One can see that the position of the critical point CP is not very sensitive to the parameter $a_{N\alpha}$. On the other hand, characteristics of PT_2 are more strongly modified in the transition between sets A and B.

A more detailed information is given in Figs. 9(a)–9(d), which represent the phase diagrams of the $\alpha - N$ matter on the (μ, T) and (n_B, T) planes. Qualitatively, the critical line of the metastable PT on the (μ, T) plane is similar to that for pure α matter [see Fig. 4(a)]. Note, however, that the end-point K cannot be regarded as a critical point. The full squares and diamonds in Fig. 9 mark, respectively, the ground states of one-component systems composed of nucleons or α's. These states coincide with the boundaries of the critical lines on the axis $T = 0$.

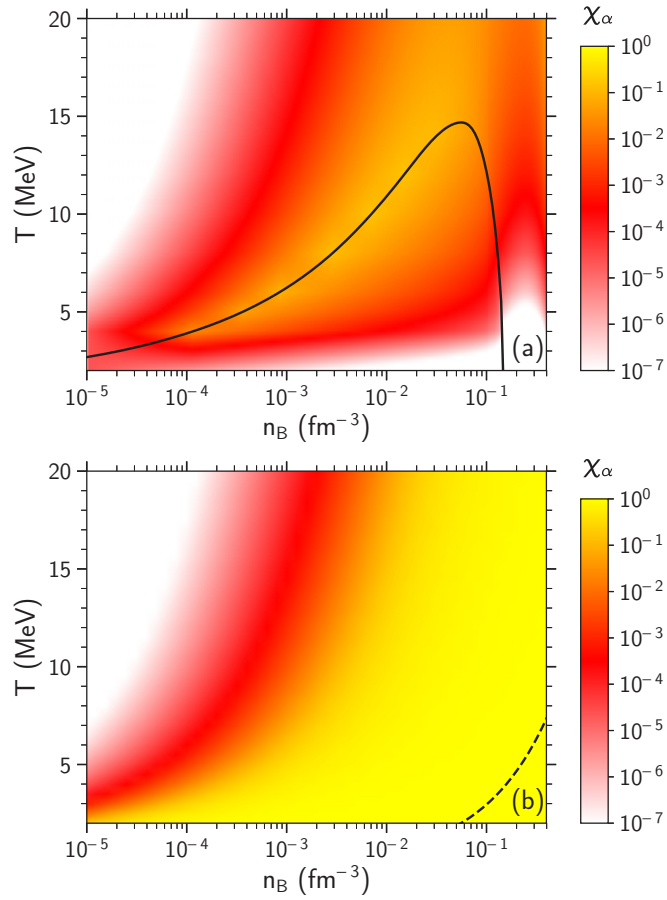

FIG. 10. (a) Contour plot of the mass fraction of α's in $\alpha - N$ matter for parameter set B. The MP boundary is shown by the solid line. (b) The same as in the upper panel but for ideal $\alpha - N$ gas. The dashed line represents the BEC boundary.

[6]This means that at $T > T_K$ there are no additional intersections between the pressure branches on the (μ, p) plane except for point PT_1. We found that pressure slopes on both sides of point PT_2 still differ when $T \to T_K$. On the other hand, the density jump disappears for transition PT_1 when $T \to T_{CP}$.

The contour plot of the mass fraction χ on the (n_B, T) plane is shown in Fig. 10(a) for parameter set B. In this calculation, we take into account only stable states of the $\alpha - N$ matter. One can see that the maximum values of $\chi \sim 0.1$–0.2 are reached near the left boundary of the LGPT.[7] At fixed temperature, χ decreases with n_B in the MP region. It is interesting that a similar nonmonotonic density behavior of χ was also predicted in Refs. [2,16,20,21,23]. We would like to emphasize that the model gives qualitatively different results as compared to the ideal $\alpha - N$ gas where the mass fraction of α's increases monotonically with n_B [see Fig. 10(b)].

V. CONCLUSIONS AND OUTLOOK

In this paper, we have analyzed the EoS and phase diagram of the chemically equilibrated $\alpha - N$ matter. Our approach simultaneously takes into account the quantum-statistical effects as well as the liquid-gas phase transitions. We apply Skyrme-like parametrizations of interaction terms as functions of particle densities. The model parameters were chosen by using the ground-state characteristics of pure nucleon and pure α matter at zero temperature. We investigate stability of the $\alpha - N$ mixture with respect to density fluctuations. The regions of possible phase transitions have been studied for different choices of model parameters. At low enough temperatures, two LGPTs are found where one is stable and the other is metastable. It is demonstrated that the phase-transition effects are important even for dilute states of the $\alpha - N$ matter. A strong suppression of α-cluster abundance is found at high nucleon densities. On the other hand, nucleon fractions are relatively small for metastable states with Bose-Einstein condensation of α's.

The results of this paper may be used for studying nuclear-cluster production in heavy-ion reactions as well as in astrophysics. To analyze dynamical processes in nuclear collisions, it would be interesting to calculate not only isotherms, but also trajectories of constant entropy per baryon. Then, one can study the possibility to reach the metastable states of α condensation in the course of isentropic expansion of excited matter produced in a heavy-ion collision.

In the present paper, we use parametrizations of mean fields which predict two separated minima of the energy per baryon of cold $\alpha - N$ matter. These minima correspond to the ground states of pure nucleon and pure α matter. Another possibility where the nuclear matter has only one ground state composed of nucleons with a small admixture of α's will be considered in a subsequent paper.

In the future, we are going to apply our approach for studies of clusterized isospin-asymmetric matter as expected in compact stars and their mergers. More realistic calculations can be performed by taking into account the Coulomb interactions as well as contributions of other light and heavy clusters. The results of this paper may be useful for investigating not only equilibrium, but also nonequilibrium mixtures of nucleons and nuclear clusters. We think that the present formalism can be also used to study the properties of binary mixtures of fermionic atoms and bosonic molecules, such as $H + H_2$ or $D + D_2$.

[7]Note that much larger relative abundances of α's and even their BECs can be reached by selecting metastable states of the $\alpha - N$ matter.

ACKNOWLEDGMENTS

I.N.M. acknowledges financial support from the Helmholtz International Center for FAIR research. The work of M.I.G. was supported by the Alexander von Humboldt Foundation and by the Goal-oriented Program of the National Academy of Sciences of Ukraine. L.M.S. acknowledges support from the Frankfurt Institute for Advanced Studies. H.St. appreciates support from the Judah M. Eisenberg Professor Laureatus of the Fachbereich Physik and the Walter Greiner Gesellschaft.

APPENDIX: THERMODYNAMIC FUNCTIONS OF THE IDEAL NUCLEON AND α GAS

Let us consider the case $\mu_\alpha < m_\alpha$ with the density of Bose-condensed α's $n_{bc} = 0$. In the lowest order in T/m_i $(i = N, \alpha)$ one gets from Eqs. (4) and (5) the relations [39],

$$n_i \simeq \frac{g_i}{\lambda_i^3(T)} \Phi^{\pm}_{3/2}\left(\frac{\mu_i - m_i}{T}\right),$$
$$p_i^{\rm id} \simeq \frac{g_i T}{\lambda_i^3(T)} \Phi^{\pm}_{5/2}\left(\frac{\mu_i - m_i}{T}\right) \quad (T \ll m_i). \tag{A1}$$

Here, upper and lower signs correspond to $i = N$ and $i = \alpha$, respectively, $\lambda_i(T)$ is the thermal wavelength introduced in Sec. II B, and

$$\Phi^{\pm}_\beta(\eta) \equiv \frac{1}{\Gamma(\beta)} \int_0^\infty \frac{x^{\beta-1} dx}{e^{x-\eta} \pm 1}, \tag{A2}$$

where $\Gamma(\beta)$ is the γ function.[8] For $\eta \leqslant 0$, one can use the decomposition in powers of fugacity: $\Phi^{\pm}_\beta(\eta) = \sum_{k=1}^\infty (\mp 1)^{(k+1)} k^{-\beta} \exp(\eta k)$. At $\eta = 0$, functions (A2) are expressed through the Riemann zeta function $\zeta(\beta)$,

$$\Phi^-_\beta(0) = \zeta(\beta), \quad \Phi^+_\beta(0) = (1 - 2^{1-\beta})\zeta(\beta). \tag{A3}$$

The classical Boltzmann approximation corresponds to the limit $\mu_i - m_i \to -\infty$. Using the approximate relation $\Phi^{\pm}_\beta(\eta) \simeq e^\eta$ at $\eta \to -\infty$ one gets, instead of Eq. (A1), much simpler relations,

$$n_i \simeq \frac{g_i}{\lambda_i^3(T)} \exp\left(\frac{\mu_i - m_i}{T}\right), \quad p_i^{\rm id} \simeq n_i T \quad \left(n_i \lambda_i^3 \ll g_i\right). \tag{A4}$$

[8]Note that $\Phi^{\pm}_\beta(\eta) = \mp Li_\beta(\mp e^\eta)$ where $Li_\beta(x) = \sum_{k=1}^\infty x^k k^{-\beta}$ is the polylogarithm of the β-th order.

[1] J. P. Bondorf, J. Phys., Colloq. **37**, C5–195 (1976); J. P. Bondorf, A. S. Botvina, A. S. Illjinov, I. N. Mishustin, and K. Sneppen, Phys. Rep. **257**, 133 (1995).
[2] J. M. Lattimer and F. D. Swesty, Nucl. Phys. A **535**, 331 (1991).
[3] H. Stöcker, G. Buchwald, G. Graebner, P. Subramanian, J. A. Maruhn, W. Greiner, B. V. Jacak, and G. D. Westfall, Nucl. Phys. A **400**, 63c (1983).
[4] J. P. Bondorf, R. Donangelo, I. N. Mishustin, C. Pethick, H. Schultz, and K. Sneppen, Nucl. Phys. A **443**, 321 (1985).
[5] G. Peilert, J. Randrup, H. Stöcker, and W. Greiner, Phys. Lett. B **260**, 271 (1991).
[6] L. M. Satarov, M. I. Gorenstein, A. Motornenko, V. Vovchenko, I. N. Mishustin, and H. Stoecker, J. Phys. G: Nucl. Part. Phys. **44**, 125102 (2017).
[7] J. W. Clark and T.-P. Wang, Ann. Phys. **40**, 127 (1966).
[8] M. T. Johnson and J. W. Clark, Kinam **2**, 3 (1980).
[9] D. M. Brink and J. J. Castro, Nucl. Phys. A **216**, 109 (1973).
[10] A. Sedrakian, H. Müther, and P. Schuck, Nucl. Phys. A **766**, 97 (2006).
[11] Ş. Mişicu, I. N. Mishustin, and W. Greiner, Mod. Phys. Lett. A **32**, 1750010 (2017).
[12] H. Horiuchi, K. Ikeda, and Y. Suzuki, Suppl. Prog. Theor. Phys. **52**, 89 (1972).
[13] I. N. Mishustin, Phys. Scr. **30**, 293 (1984).
[14] A. Tohsaki and N. Itagaki, arXiv:1809.00460.
[15] C. J. Horowitz and A. Schwenk, Nucl. Phys. A **776**, 55 (2006).
[16] V. Vovchenko, A. Motornenko, P. Alba, M. I. Gorenstein, L. M. Satarov, and H. Stoecker, Phys. Rev. C **96**, 045202 (2017).
[17] A. S. Botvina and I. N. Mishustin, Nucl. Phys. A **843**, 98 (2010).
[18] N. Buyukcizmeci *et al.*, Nucl. Phys. A **907**, 13 (2013).
[19] S. Furusawa and I. Mishustin, Phys. Rev. C **97**, 025804 (2018).
[20] M. Hempel and J. Schaffner-Bielich, Nucl. Phys. A **837**, 210 (2010).
[21] H. Pais, F. Gulminelli, C. Providência, and G. Röpke, Phys. Rev. C **97**, 045805 (2018).
[22] S. Typel, J. Phys. G: Nucl. Part. Phys. **45**, 114001 (2018).
[23] S. Lalit, M. A. A. Mamun, L. Constantinou, and M. Prakash, Eur. Phys. J. A **55**, 10 (2019).
[24] X.-H. Wu, S.-B. Wang, A. Sedrakian, and G. Röpke, J. Low Temp. Phys. **189**, 133 (2017).
[25] D. Anchishkin, Zh. Eksp. Teor. Fiz. **102**, 369 (1992) [Sov. Phys. JETP **75**, 195 (1992)].
[26] D. Anchishkin and E. Suhonen, Nucl. Phys. A **586**, 734 (1994).
[27] L. M. Satarov, M. N. Dmitriev, and I. N. Mishustin, Phys. At. Nucl. **72**, 1390 (2009).
[28] M. Bender, P.-H. Heenen, and P.-G. Reinhard, Rev. Mod. Phys. **75**, 121 (2003).
[29] J. R. Stone, N. J. Stone, and S. A. Moszkowski, Phys. Rev. C **89**, 044316 (2014).
[30] L. D. Landau and E. M. Lifshitz, *Statistical Physics* (Pergamon, Oxford, 1975).
[31] L. M. Satarov, K. A. Bugaev, and I. N. Mishustin, Phys. Rev. C **91**, 055203 (2015).
[32] L. M. Satarov, V. Vovchenko, P. Alba, M. I. Gorenstein, and H. Stoecker, Phys. Rev. C **95**, 024902 (2017).
[33] H. Müller and B. D. Serot, Phys. Rev. C **52**, 2072 (1995).
[34] *Theory and Simulation of Hard Sphere Fluids and Related Systems*, edited by A. Mulero, Lecture Notes in Physics Vol. 753 (Springer, Berlin, 2008).
[35] W. Greiner, L. Neise, and H. Stöcker, *Thermodynamics and Statistical Mechanics* (Springer, Berlin, 1997).
[36] G. Röpke, L. Münchov, and H. Schulz, Nucl. Phys. A **379**, 536 (1982).
[37] W. Reisdorf *et al.* (FOPI Collaboration), Nucl. Phys. A **848**, 366 (2010).
[38] K. Schmidt *et al.*, Phys. Rev. C **95**, 054618 (2017).
[39] Yu. M. Poluektov and A. A. Soroka, arXiv:1709.09698.